FABRICATION AND CHARACTERISATION OF XANTHAN GUM- GELATINE BLEND NANOFIBERS/PARTICLES PRODUCED BY ELECTROSPINNING METHOD

ECEM DOGAN[1,2*] , MUSTAFA SENGOR[1,3,4], OGUZHAN GUNDUZ[1,3,4], CEM BULENT USTUNDAG[2,4]

[1] *Center for Nanotechnology & Biomaterials Application and Research (NBUAM), Marmara University, Istanbul, Türkiye*
[2] *Department of Bioengineering, Faculty of Chemical and Metallurgical Engineering, Yildiz Technical University, Istanbul, Türkiye*
[3] *Department of Metallurgical and Materials Engineering, Faculty of Technology, Marmara University, Istanbul, Türkiye*
[4] *Health Biotechnology Joint Research and Application Center of Excellence, 34220 Esenler, Istanbul, Türkiye*

This study aims to obtain nanoparticles by electrospinning method using xanthan gum (XG) and gelatine (GEL) polymers. For the development of these nanoparticles, ten different groups were produced. In some groups, nanofiber was obtained instead of particles. The nanofiber formation was determined in the 10 wt% GEL, 12 wt% GEL, 3 wt% XG, 8 wt% GEL + 3 wt% XG. 12 wt% GEL + 0.1 wt% XG groups. 4 wt% GEL + 1 wt% XG and 8 wt% GEL + 3 wt% XG groups showed nanoparticles structure. To assess the nanofibers chemical properties, Fourier transform infrared spectroscopy (FTIR) were used. Scanning electron microscopy (SEM) was used to characterize mechanical and morphological properties. Physical properties and swelling behaviours were examined to analyse the samples. As a result of the swelling test, 3 wt% XG was degraded, 10 wt% and 12 wt% gelatin groups started to degrade after the fourth day. Our work deduced that GEL/XG nanoparticles could use for carrier purposes. Also, this study was beneficial in finding the right ratios in the production of nanoparticles and nanofibers from the XG/GEL mixture by electrospinning. In addition, proper electrospinning parameters in nanofiber and nanoparticles production are also important results of the study and will be further used in developing composite nanostructures with regenerative or drug release capability.

Keywords: *gelatin; xanthan gum; electrospinning; particle; fiber*

1. Introduction

Nanofibers produced by the electrospinning method allows polymer fibers to form between a few nanometers and a few microns. This technique has been widely used in recent years. Reasons for the preference of nanofibers are that they can be produced easily by electrospinning, which is an inexpensive technique, their surface area is large, their mechanical properties and diameters are adjustable, surface with high porosity and nanoscale dimensions, successfully employed in a variety of medical applications, including antibacterial dressing (1), wound dressing (2), scaffolds and artificial organ (3). Fibrous structures are not as good for drug delivery systems as nanoparticles. Therefore, a uniform beadless nanofiber structure can be used in protective clothing, drug delivery systems, or additive (4). Drug loading capacity can be regulated by particle sizes. In this way, the nanoparticles can be used as drug carriers (5).

With the electrospinning method, nanofibers can be produced different morphologies and smooth from different polymers (6, 7, 8). In this method, nanofibers are obtained from polymers by applying an electric field. In the electrospinning technique, nanofibers with different morphologies can be produced by changing parameters such as voltage, distance, feed rate and concentration (9, 10). Nanofiber diameters are also one of the critical parameters in the electrospinning technique. As the viscosity increased, it was determined that a larger nanofiber diameter was obtained (11, 12).

Gelatine (gel), which is a natural polymer and has hydrophilic properties, is a commercially produced polypeptide from the hydrolysis of collagen, and it is simple to obtain and inexpensive (13, 14). Also, gelatine and its derivatives have properties such as non-toxic, biocompatibility and biodegradability. Due to these properties, gelatine can be used in the scaffold in tissue engineering, in synthesizing bio composites containing a variety of chemicals, including medicines and nanoparticles (15). In a study, it was reported that fibroblasts grow well on gelatine nanofibers. According to these results, it was stated that gelatine predicted to provide important structural and chemical hints and valuable in tissue engineering and regenerative medicine (16). In addition to these areas, gelatine has been used in drug delivery applications (17, 18,19).

Xanthan gum (XG) is a heteropolysaccharide obtained from the bacterium *Xanthomonas campestris* (20, 21). XG consists of the main chain with β1-4-linked and repeating D-glucose units and a side chain of D-mannose and D-glucuronic acid. It can be compatible with metallic salts, showing stability at different pH levels, temperatures and high viscosity at low concentrations (21). XG, which can be used in medicine and pharmacology thanks to its biocompatibility, bio-adhesiveness and wound healing properties, has been approved by the FDA thanks to these properties (22). XG is growingly employed for the development and enhancement of drug delivery systems due to its physicochemical features (23). XG has been used for many biomedical and pharmaceutical purposes such as antiviral carriers, antibacterial carriers, anticancer

*Autor corespondent/*Corresponding author*,
E-mail: eccemdogan@gmail.com

drugs, controlled-release tablets and hydrogels for the administration of various drugs with successful results (24, 25, 26, 27, 28).

Recent studies have shown that gelatine/xanthan gum bioprinted hydrogels are biocompatible materials as they allow the growth of both human keratinocyte and fibroblast in vitro (29). In another study, gelatine-based nanofibers have been strengthened using oxidized xanthan gum (OXG) as a crosslinking agent because of the high hydrophilicity and poor mechanical properties of gelatine for food packaging (30). In a different study, rotatable and electroresponsive polyelectrolyte hydrogels prepared XG and gelatine were prepared at different ratios. XG-Gelatine5 (5 wt%) hydrogels were determined to have higher strength and critical stress than those of XG hydrogels. It has been observed that XG-Gelatine5 hydrogels release ciprofloxacin (CPFX) gradually in a controlled manner in neutral and acid environment at 37°C (31). Also, in the literature, in order to form a new natural and biodegradable composite film for food packaging industry, gelatine-carboxymethyl cellulose (CMC)-xanthan gum films were obtained by mixing the gelatine-carboxymethyl cellulose (CMC) mixture as XG crosslinking agent in different ratios and the gelatine-CMC film containing 5% xanthan gum showed better physical and mechanical properties than other films (32).

This study, it was aimed to obtain GEL/XG nanoparticles that can serve as drug delivery systems as carriers and optimize the suitable concentrations for GEL/XG particles. GEL, XG, GEL/XG nanofibers and nanoparticles were produced by the electrospinning technique. Physical (density, viscosity, and surface tension), morphological, chemical, and mechanical properties of prepared scaffolds were evaluated utilizing various characterisation techniques. Also, swelling behaviors were studied. This study shows that GEL/XG nanoparticles can be obtained by electrospinning technique and these nanoparticles can be used as drug carriers and by adding XG to gelatine as an additive in various applications. This study also shows in what proportions nanoparticles can be obtained and in what proportions nanofibers are not formed from the XG/GEL mixture.

2. Materials and Methods

2.1. Materials

Gelatine from porcine skin (~300 bloom; type A) were purchased from Sigma-Aldrich, USA. Xanthan gum was bought from Yasin Teknik Company. Molecular weight of xanthan gum is 933.7462 g/mol. Glutaraldehyde and tween-80 (surfactant) were purchased from Sigma Aldrich, Germany.

2.2. Solution preparation

GEL, XG, and GEL/XG solutions in various concentrations were made, and their composition is shown in Table 1. 8 wt% GEL, 10 wt% GEL, 12 wt% GEL, 1 wt% XG, 2 wt % XG, 3 wt % XG, 4 wt % XG, 4 wt% GEL + 1 wt% XG, 8wt% GEL + 3 wt% XG, 12 wt% GEL + 0.1 wt% XG were prepared by dissolving in 10 ml formic acid with a magnetic stirrer and 2 drops Tween-80. GEL groups stirred 2 h at room temperature, XG groups stirred 4 h at 70 °C and GEL/XG groups stirred overnight at 40 °C.

2.3. Fabrication of the fibers and particles via electrospinning

The nanofibers were fabricated using electrospinning method. Different electrospinning parameters tested to obtain bead-free smooth fiber. These parameters are flow rate, needle–collector distance, polymer concentration, applied voltage.

Table 1

Content of solutions

Groups	Gelatin content (Wt %)	Xanthan Gum content (Wt %)
GEL-8	8	0
GEL-10	10	0
GEL-12	12	0
XG-1	0	1
XG-2	0	2
XG-3	0	3
XG-4	0	4
GEL-4 + XG-1	4	1
GEL-8 + XG-3	8	3
GEL-12 + XG-0.1	12	0.1

Polymer solutions were injected into a 10 mL syringe that was connected to a 27-gauge needle. The collector was 10 centimeters away from the needle tip. Applied voltage and flow rate were 0.1 ml/h and 24 kV for 8 wt% GEL, 0.1 ml/h and 20.4 kV for 10 wt% GEL, 0.5 ml/h and 19.1 kV for 12 wt% GEL solution, 0.6 ml/h and 28.5 kV for 2 wt% XG, 0.3 ml/h and 29.9 kV for 3 wt% XG, 0.2 ml/h and 31.9 kV for 8 wt% GEL + 3 wt% XG solution and 0.3 ml/h and 32.5 kV for 12 wt% GEL + 0.1 wt% XG solution, respectively. Random nanofibers were collected on the surface of a rectangular piece of parchment on the collector and rotated at 15 rpm. The nanofibers were then removed from the parchment paper and kept at room temperature. 10 wt% GEL, 12 wt% GEL and 3 wt % XG groups were crosslinked via glutaraldehyde (GA) vapor for 2 hours. A 35x10 mm glass plate was utilized and filled with a solution of Glutaraldehyde. The plate was then positioned at the bottom of a desiccator. The nanofibers were carefully placed on top of the glass chamber, and the entire apparatus was subsequently placed inside an incubator that was set to maintain a temperature of 60°C.

2.4. Characterisation of the physical properties of solutions and nanofibers

In order to determine the physical properties of the prepared polymer solutions, a force tensiometer (Sigma 703D, Attention, Germany) was used to conduct surface tension tests. The viscosity of the polymer solutions was measured at room temperature using a digital viscometer (DV-E, Brookfield AMETEK, USA). To obtain density measurements, a Gay Lussac standard density bottle (10 ml) (Boru Cam, Turkey) was employed in accordance with DIN ISO 3507. Conductivity of the prepared solutions was characterized using an electroconductive meter (Cond 3110 SET 1 WTW, Germany). Equipments were calibrated and all tests carried out three times. Nanofibers molecular composition and chemical characterization were examined using Fourier transform infrared spectroscopy at scanning range between 450 and 4000 cm^{-1} (FTIR 4700, Jasco, Japan). Scanning electron microscopy was used to analyze the surface morphology of nanofibers and nanoparticles (SEM) (EVA MA 10, ZEISS, USA). A sputter coating machine was used to cover the surface of the samples with gold (Au) for 120 seconds prior to imaging (Quorum SC7620, ABD). The morphological characteristics and pore size differences of each nanofiber and nanoparticle were examined. The pore sizes of both the nanofibers and nanoparticles were measured using software (Analysis5, Olympus, USA), and the average pore size was determined for each sample. The swelling properties of the nanofibers were examined over the course of five days. On the first day, the initial weights (W0) of the nanofibers were recorded, following which all the nanofibers (10 wt% GEL, 12 wt% GEL, 3 wt % XG) were placed in 1 ml phosphate buffer saline (PBS) with pH 7.4. The nanofibers were then subjected to a thermal shaker (BIOSAN TS-100) set to a temperature of 37°C, and subsequently removed for analysis. Filter paper was used to absorb and remove the surplus water. To perform the swelling test, the wet weights (Ww) of the samples were recorded daily for five consecutive days (1, 2, 3, 4, 5). The swelling value (S) was then determined using equation (eq 1).(33).

$$S = \frac{(W_w - W_o)}{W_o} . 100$$

A tensile test equipment was used to determine the nanofibers tensile strength (SHIMADZU, EZ-LX, CHINA). Process was carried out at a crosshead speed of 5 mm/s at room temperature (n = 5). The nanofiber thickness was measured using a digital micrometer (Mitutoyo MTI Corp., USA). Samples were sliced into rectangles of 50 mm in length and 10 mm in breadth.

3. Results and discussion

GEL, XG and GEL/XG solutions were prepared in different ratios to obtain nanofibers by electrospinning method. It has been stated in the literature that the technique and 3D printer parameters, which included 2.5 w/v% and 3 w/v% gelatine and 1.2 w/v% xanthan gum, resulted in a printable, high-resolution model (34). In another study, it was stated that to evaluate skin wound healing efficacy XG, GEL, citric acid (c) and GA with different proportions were dispersed in HPLC-grade water for the preparation of hydrogels with different compositions. XG (600 mg):GEL (3 mg):GA (0.5 ml), XG (600 mg): GEL(5 mg):GA (0.5 ml), and XG (600 mg):C (30 mg):GEL(5 mg):GA (0.5 ml) treated wounds showed highest recovery (35). Physical parameters of the solutions were characterised and optimized, including density, viscosity, electrical conductivity, and surface tension. Also sizes of the particles were calculated (Table 2). It was observed that the electrical conductivity and surface tension were maximum in the 8 wt% GEL+ 3 wt% XG group. It was determined that 12 wt% GEL+ 0.1 wt% XG and 4 wt% groups have the largest sizes as particles.

The chemical structures of varied ratios of GEL and XG nanofibers were investigated using FTIR analysis. Figure 1 shows a graphical representation of the results. The spectrum of gelatine revealed multiple characteristic bands. The peak at 3300 cm^{-1} indicates the presence of hydrogen bond water and amide-A due to the N-H stretching, the peak at 1630 cm^{-1} indicates amide-I due to the C=O stretching vibrations, the peak at 1565 cm^{-1} indicates amide-II and the peak at 1240 cm^{-1} indicates the amide-III (36, 37) . The peak at 1730 cm^{-1}, due to C=O stretching of the xanthan acetate group. The peak indicates from 1700 and 1600 cm^{-1} due to xanthan O–H angular

Table 2

Physical properties of the solution and sizes of the beads

Groups	Surface tension (mN/m)	Viscosity (mPa.s)	Density (kg/m³)	Conductivity (ms/cm)	Particles Sizes (µm)
GEL-8	19.6 ± 0.94	70.8 ± 0.31	1.211	2.6 ± 0.005	1
GEL-10	19.8 ± 0.61	104.6 ± 0.40	1.213	3.15 ± 0.035	-
GEL-12	18.3 ± 0.41	147.9 ± 0.3	1.214	1.5 ± 0.010	-
XG-1	20.37 ± 0.23	6.7 ± 0.05	1.233	0.9 ± 0.0020	25.5
XG-2	18.2 ± 0.17	1157.6 ± 0.01	1.192	1.6 ± 0.016	25.9
XG-3	19.98 ± 0.35	65.3 ± 1266	1.208	0.7 ± 0.039	-
XG-4	21.39 ± 0.66	28.9 ± 10.94	1.191	2.3± 0.127	86.7
GEL-4 + XG-1	34.13 ± 0.51	23.38 ± 0.05	1.206	2.09 ± 0.015	1
GEL-8 + XG-3	80.3 ± 13.71	194.6 ± 73.24	1.201	4.01 ± 0.011	-
GEL-12 + XG-0.1	31.9 ± 0.57	3498.6 ±24.70	1.213	3.6 ± 0.023	317.8

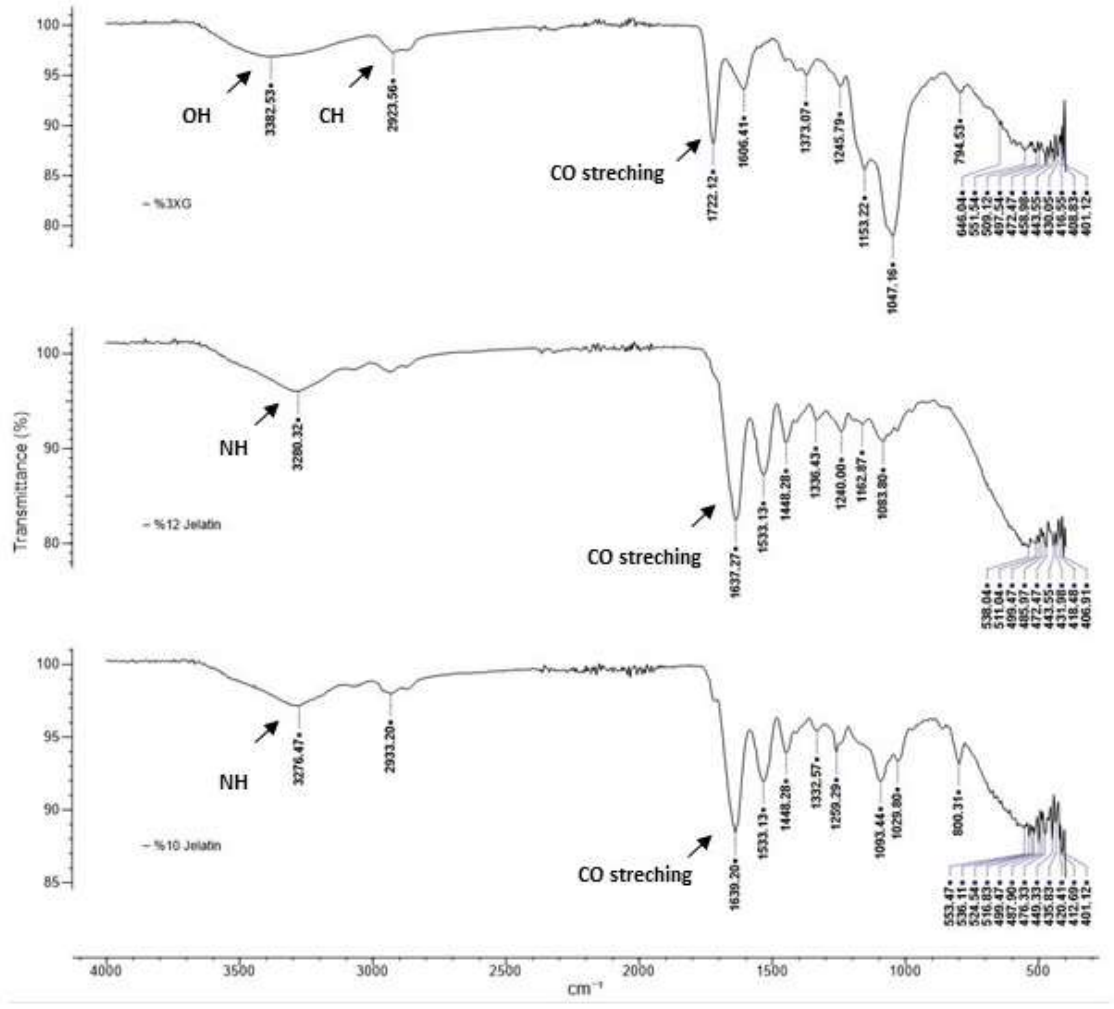

Fig. 1 - FTIR spectroscopy of GEL and XG fibers

deformation, the proteins amide I band and symmetric stretching of carboxylate group of pyruvate and of glucuronic acid. The peak indicates from 1100 and 900 cm^{-1} to xanthan C–O stretching. The bands around 3400 cm^{-1}, 2939 cm^{-1} and 990–1200 cm^{-1} indicates O–H bonds, C–H bonds of CH2 groups and saccharides, respectively (38)

GEL, XG nanofibers and GEL/XG nanoparticles were produced by electrospinning. Diameters of the nanofibers produced by this method are very significant according to the application areas that they are actively used.

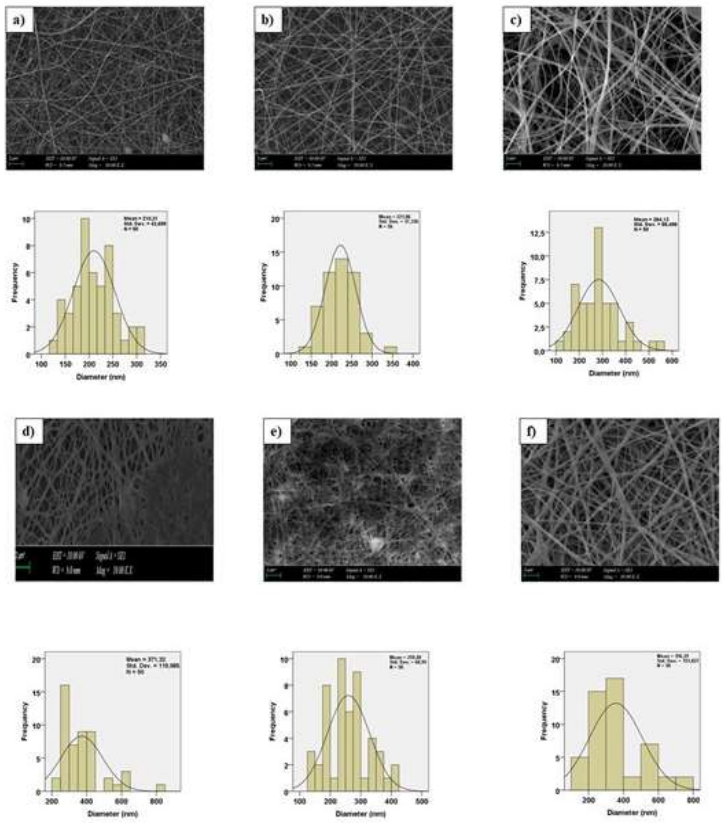

Fig. 2 - SEM images and pore size histograms of 10 wt% GEL (a), 12 wt% GEL (b) and 3 wt% XG (c) nanofibers before crosslink, and 10 wt% GEL (d), 12 wt% GEL (e) and 3 wt% XG (f) nanofibers after the crosslink, respectively

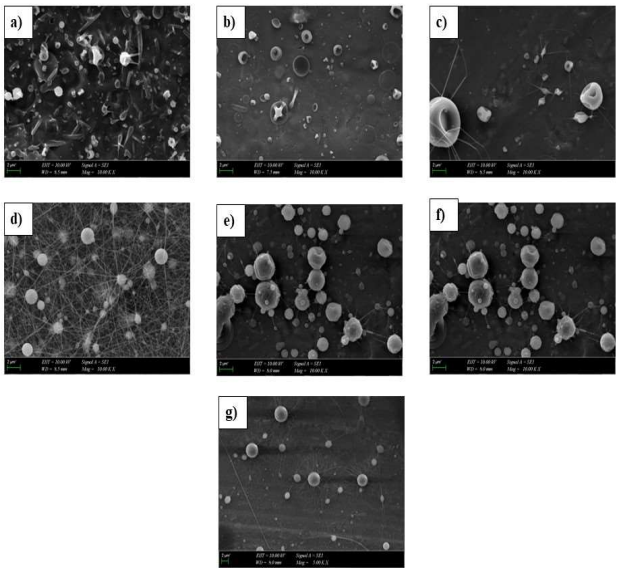

Fig. 3 - SEM images of electrospun particles with varying polymer solution concentrations: 1 wt% XG (a), 2 wt% XG (b), 4 wt% XG (c), 8 wt% GEL (d), 4 wt% GEL + 1 wt% XG (e), 8 wt% GEL + 3 wt% XG (f), and 12 wt% GEL + 0.1 wt% XG (g), respectively

Results show that average nanofiber size distributions of 10 wt% GEL resulted in 210.31 µm. After the crosslinking the distribution resulted in 371.32 µm. Average nanofiber size distributions for 12 wt% GEL and 3 wt% XG resulted in 221.86 µm and 284.13 µm, respectively. After the crosslinking the distribution for 12 wt% GEL and 3 wt% XG resulted in 259.48 µm and 356.29 µm, respectively. The average nanofiber size distributions increase after crosslinking for 3% XG, 10%, and 12% GEL. In the literature, it has been stated that the average diameters of 7-12 wt% gelatin solutions dissolved in 98% formic acid vary between 70 and 170 µm. Our nanofibers were thicker than those reported in the

literature (39). SEM images of each nanofiber and their sizes histogram were shown in fig. 2 (a), (b), (c), (d), (e), (f). We demonstrated that the diameters of the nanofibers increased after cross-linking and the highest nanofiber diameter was in 3 wt% XG group before crosslinking and 10 wt% gelatin group after crosslinking. Nanofiber could not be obtained in 1 wt%, 2 wt% and 4 wt% XG and 8 wt% GEL groups. Also, we observed that nanofiber could be obtained after optimizing the GEL and XG groups, but could not be obtained from the GEL/XG groups and nanoparticles were formed (Fig. 3 (a), (b), (c), (d), (e), (f), (g)). In the GEL/XG groups, nanofiber was formed only in the 8 wt% GEL + 3 wt% XG group, but it was observed that nanoparticles were formed when collected. We concluded that there is a relationship between solution density and formation pattern of nanoparticles apart from nanofibers in these groups. It has been observed that the formation of nanoparticles instead of nanofibers in these groups is related to the solution densities. Also, it has been observed that the voltage and distance, together with the solution density, have an effect on the formation of nanofibers and nanoparticles in different groups. Additionally, the voltage and distance parameters together with solution density, influenced the formation of nanofibers and nanoparticles in different groups

Swelling feature of the nanofibers is also an important parameter in the utilization of many applications. It has been stated in previous studies that swelling ability increases mechanical flexibility (40). In addition, it has been reported that the swelling rates of porous scaffolds decrease at low gelatine contents (41). 3% XG group demonstrated immediate degradation behavior. The both 10 wt% and 12 wt% GEL groups reached the highest swelling rate up to near 400%. It was observed that both groups had a decrease in swelling rates after the fourth day (fig. 4).

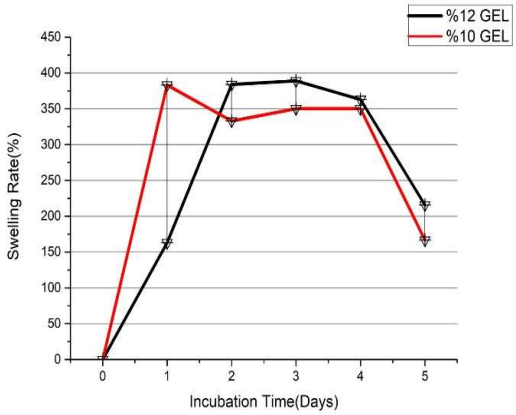

Fig. 4 - Swelling ability of 10 wt% GEL and 12 wt% GEL

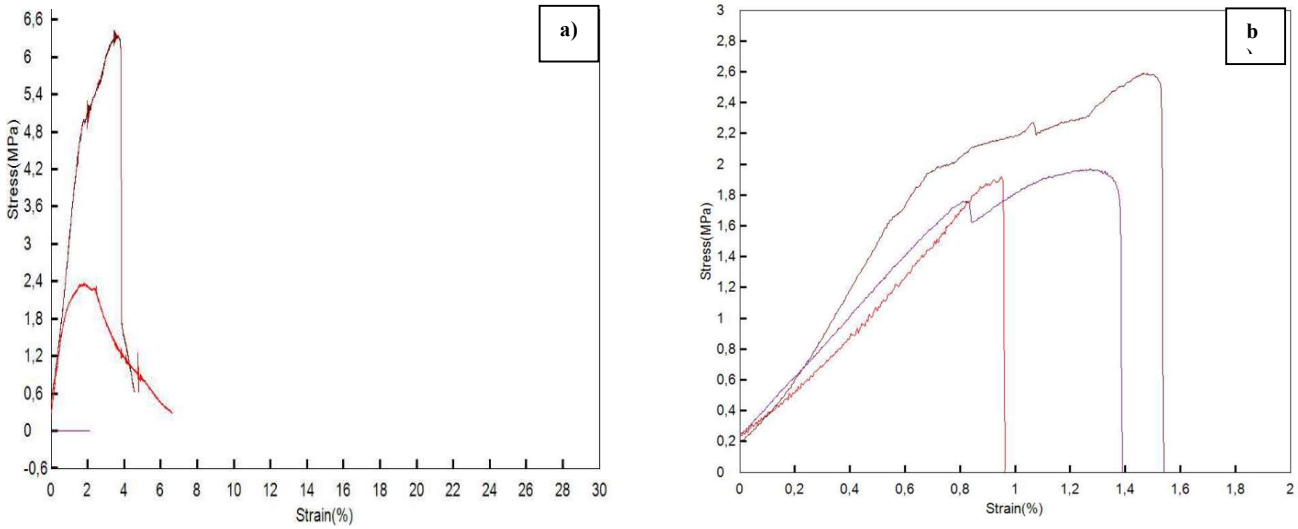

Fig. 5 continues on next page

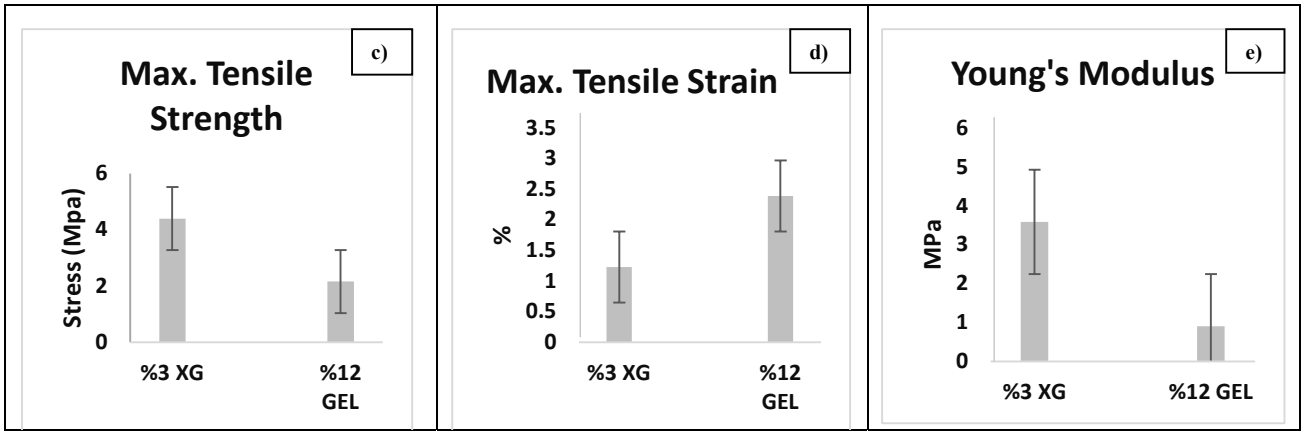

Fig. 5 - Stress- strain graphics of 3 wt% XG (a) and 12 wt% GEL (b) and max. tensile strength (c), max. tensile strain (d) and young's modulus (e) graphics of 3 wt% XG and 12 wt% GEL, respectively (origin pro)

Table 3

Stress- strain values of 3 wt% XG (a) and 12 wt% GEL (b)

Groups	3 wt% XG	12 wt% GEL
Max. stress (MPa)	2.93 ± 3.25	2.15 ± 0.37
Max. strain (%)	2.39 ± 0.92	1.23 ± 0.26

Uniaxial tensile testing was performed on the nanofibers to test the mechanical proporties. Important factors in tensile testing are tensile strength and elongation at break. The tensile stress–strain curves of the electrospun nanofibers are presented in Fig. 5. It was determined that the maximum tensile strength and the maximum young's modulus value is in the 3% XG group and the maximum tensile strain value is in the 12 wt% GEL group. It has been determined by tests that the mechanical strengths of the XG and GEL groups are not the same (Table 3). It has been stated that the stress-strain curves for gelatine nanofiber is zig-zag, due to interfiber shear or small-scale tensile insufficiency in subsets of fibers (42) .

4. Conclusion

Electrospinning is a simple and adaptable technique for making nanoscale threads from a variety of materials, including metals, ceramics, and polymers. In this study, GEL and XG nanofibers and GEL/XG nanoparticles at different ratios with electrospinning method have been produced successfully. GEL and XG were used because of their important properties such as biocompatibility in biomedical and other fields. By using different ratios of GEL and XG, the most accurate ratios were found and electrospinning method nanofibers were produced successfully. It was observed that 3 wt% XG was degraded in the first hour in the swelling test and cannot be used alone in biomedical or food applications. GEL and XG groups formed nanofibers separately by electrospinning but when mixed in different proportions, they formed nanoparticle structures. It was observed that only 3 wt% concentration was formed nanofiber in the XG group. For GEL groups, 10 wt% and 12 wt% concentrations were formed nanofiber. For GEL/XG blend groups 4 wt% GEL + 1 wt% XG and 8 wt% GEL + 3 wt% XG and 12 wt% GEL + 0.1 wt% XG concentrations were formed nanoparticles and nanofiber structure was not observed in these groups. Consequently, GEL/XG blend nanoparticles can be used for drug carrier or by adding XG to gelatin as an additive in various applications such as food industry.

REFERENCES

[1] S. Homaeigohar, A. R. Boccaccini, Antibacterial biohybrid nanofibers for wound dressings, Acta biomaterialia, 2020, 107, 25.

[2] A. Zarghami, M. Irani, A. Mostafazadeh, et al., Fabrication of PEO/chitosan/PCL/olive oil nanofibrous scaffolds for wound dressing applications, Fibers and Polymers, 2015, 16, 1201.

[3] M. R. Ramezani, Z. Ansari-Asl, E. Hoveizi, et al., Fabrication and Characterization of Fe(III) Metal-organic Frameworks Incorporating Polycaprolactone Nanofibers: Potential Scaffolds for Tissue Engineering, Fibers and Polymers, 2020, 21, 1013.

[4] P. Ruenraroengsak, J. M. Cook, and A. T. Florence, Nanosystem drug targeting: Facing up to complex realities, Journal of Controlled Release, 2010, 141 (3), 265.

[5] X. Hong, M. Edirisinghe, S. Mahalingam, Beads, beaded-fibres and fibres: Tailoring the morphology of poly(caprolactone) using pressurised gyration, Materials Science and Engineering: C, 2016, 69, 1373.

[6] V. Beachley, E. Katsanevakis, N. Zhang, et al., Highly aligned polymer nanofiber structures: Fabrication and applications in tissue engineering, 2012, 246, 171.
[7] H. Matsumoto, A. Tanioka, Functionality in electrospun nanofibrous membranes based on fiber's size, surface area, and molecular orientation, Membranes, 2011, 1 (3), 249.
[8] J. Lin, X. Wang, B. Ding, et al., Biomimicry via electrospinning, Critical Reviews in Solid State and Materials Sciences, 2012, 37 (2), 94.
[9] D. H. Reneker, W. Kataphinan, A. Theron, et al., Nanofiber garlands of polycaprolactone by electrospinning, Polymer, 2002, 43 (25), 6785.
[10] Y. Xin, D. H. Reneker, Garland formation process in electrospinning, Polymer, 2012, 53 (16), 3629.
[11] P. K. Baumgarten, Electrostatic spinning of acrylic microfibers, Journal of Colloid and Interface Science, 1971, 36 (1), 71.
[12] J. Doshi, D. H. Reneker, Electrospinning process and applications of electrospun fibers, Journal of electrostatics, 1993, 3, 1698.
[13] N. Detta, C. Errico, D. Dinucci et al., Novel electrospun polyurethane/gelatin composite meshes for vascular grafts, Journal of Material Science: Materials in Medicine, 2010, 21, 1761.
[14] C. L. Tseng, T. W. Wang, G. C. Dong et al., Development of gelatin nanoparticles with biotinylated EGF conjugation for lung cancer targeting, Biomaterials, 2007, 28 (27), 3996.
[15] F. Han, Y. Dong, Z. Su, et al., Preparation, characteristics and assessment of a novel gelatin-chitosan sponge scaffold as skin tissue engineering material, International Journal of Pharmaceutics, 2014, 476, 1, 124.
[16] H. Aoki, H. Miyoshi, Y. Yamagata, Electrospinning of gelatin nanofiber scaffolds with mild neutral cosolvents for use in tissue engineering, Polymer Journal, 2015, 47, 3, 267.
[17] N. Zandi, R. Lotfi, E. Tamjid, et al., Core-sheath gelatin based electrospun nanofibers for dual delivery release of biomolecules and therapeutics, Materials Science and Engineering: C, 2020, 108, 110432.
[18] M. Gaydhane, P. Choubey, C. S. Sharma, et al., Gelatin nanofiber assisted zero order release of Amphotericin-B: A study with realistic drug loading for oral formulation, Materials Today Communications, 2020, 24, 100953.
[19] B. Jiang, Z. Yang, H. Shi, et al., Potentiation of Curcumin-loaded zeolite Y nanoparticles/PCL-gelatin electrospun nanofibers for postsurgical glioblastoma treatment, Journal of Drug Delivery Science and Technology, 2023, 80, 104105.
[20] A. C. Mendes, E. T. Baran, R. C. Pereira, et al., Encapsulation and Survival of a Chondrocyte Cell Line within Xanthan Gum Derivative, Macromolecular Bioscience, 2012, 12 (3), 350.
[21] G. Han, G. Wang, X. Zhu, et al., Preparation of xanthan gum injection and its protective effect on articular cartilage in the development of osteoarthritis, Carbohydrate Polymers, 2012, 87 (2), 1837.
[22] A. Kumar, K. M. Rao, S. S. Han, Application of xanthan gum as polysaccharide in tissue engineering: A review, Carbohydrate Polymers, 2018, 180, 128.
[23] H. Cortes, I. H. Caballero- Floran, N.Mendoza-Munoz et al., Xanthan gum in drug release, Cellular and Molecular Biology, 2020, 66 (4),199.
[24] N. S. Malik, M. Ahmad, M. U. Minhas, et al., Chitosan/Xanthan Gum Based Hydrogels as Potential Carrier for an Antiviral Drug: Fabrication, Characterization, and Safety Evaluation, Frontiers in Chemistry, 2020, 8, 50.
[25] S. Hauschild, U Lipprandt, A. Rumplecker et al., Direct preparation and loading of lipid and polymer vesicles using inkjets, Small, 2005, 1 (12), 1177.
[26] N. M. El-Sawy, A. I. Raafat, N. A. Badawy, et al., Radiation development of pH-responsive (xanthan-acrylic acid)/MgO nanocomposite hydrogels for controlled delivery of methotrexate anticancer drug, International Journal of Biological Macromolecules, 2020, 142, 254.
[27] D. A. Fara, S. M. Dadou, I Rashid, et al., A direct compression matrix made from xanthan gum and low molecular weight chitosan designed to improve compressibility in controlled release tablets, Pharmaceutics, 2019, 11 (11), 603.
[28] L. Djekic, M. Martinović, V. Dobričić, et al., Comparison of the Effect of Bioadhesive Polymers on Stability and Drug Release Kinetics of Biocompatible Hydrogels for Topical Application of Ibuprofen, Journal of. Pharmaceutical Sciences, 2019, 108 (3), 1326.
[29] B. Piola, M. Sabbatini, S. Gino, et al., 3D Bioprinting of Gelatin–Xanthan Gum Composite Hydrogels for Growth of Human Skin Cells, International Journal of Molecular Sciences, 2022, 23 (1), 539.
[30] L. Y. Maroufi, R. Norouzi, S. Ramezani, et al., Novel electrospun nanofibers based on gelatin / oxidized xanthan gum containing propolis reinforced by Schiff base cross-linking for food packaging, Food Chemistry, 2023, 416, 135806.
[31] Q. Xu, Y. Zhang, R. Zhang, et al., Electroresponsive and spinnable hydrogels from xanthan gum and gelatin enhanced by Fe3+ ions coordination, Journal of Applied Polymer Science, 2021, 138 (48), 51601.
[32] M. A. S. P. Nur Hazirah, M. I. N. Isa, N. M. Sarbon, Effect of xanthan gum on the physical and mechanical properties of gelatin-carboxymethyl cellulose film blends, Food Packaging and Shelf Life, 2016, 9 (55).
[33] S. N. Alhosseini, F. Moztarzadeh, M. Mozafari, et al., Synthesis and characterization of electrospun polyvinyl alcohol nanofibrous scaffolds modified by blending with chitosan for neural tissue engineering, International Journal of Nanomedicine, 2012, 7, 25.
[34] B. Piola, M. Sabbatini, S. Gino, et al., 3D Bioprinting of Gelatin–Xanthan Gum Composite Hydrogels for Growth of Human Skin Cells, International Journal of Molecular Sciences, 2022, 23 (1), 539.
[35] M. M. A. K. Shawan, N. Islam, S. Aziz, et al., Fabrication of Xanthan gum: Gelatin (Xnt:Gel) Hybrid Composite Hydrogels for Evaluating Skin Wound Healing Efficacy, Modern Applied Science, 2019, 13 (3), 101.
[36] S. Unal, S. Arslan, T. Gokce, et al., Design and characterization of polycaprolactone-gelatin-graphene oxide sca ff olds for drug influence on glioblastoma cells, European Polymer Journal, 2019, 115, 157.
[37] Z. A. Nur Hanani, Y. H. Roos, J. P. Kerry, Fourier Transform Infrared (FTIR) spectroscopic analysis of biodegradable gelatin films immersed in water, in 11th International Congress on Engineering and Food, 2011, p 22.
[38] D. Osiro, R. W. A. Francoa, L. A. Colnago, Spectroscopic characterization of the exopolysaccharide of Xanthomonas axonopodis pv. citri in Cu2+ resistance mechanism, Journal of the Brazilian Chemical Society, 2011, 22, 1339.
[39] N. Choktaweesap, K. Arayanarakul, D. Aht-Ong, et al., Electrospun gelatin fibers: Effect of solvent system on morphology and fiber diameters, Polymer Journal, 2007, 39 (6), 622.
[40] Y. Gao, W. Kong, B. Li, et al., Fabrication and characterization of collagen-based injectable and self-crosslinkable hydrogels for cell encapsulation, Colloids and Surfaces B:Biointerfaces, 2018, 167, 448.
[41] V. T. Nguyen, S. Chun Ko, G. Woo Oh, et al., Anti-inflammatory effects of sodium alginate/gelatine porous scaffolds merged with fucoidan in murine microglial BV2 cells, International Journal of Biological Macromolecules, 2016, 93,1620.
[42] O. A. Journal, Biointerface Research in Applied Chemistry, 2020, 10 (3), pp. 5556.

****